LANGMUIR

N-Heterocyclic Carbene Ligands for Au Nanocrystal Stabilization and Three-Dimensional Self-Assembly

Sylvain Roland,*,† Xiang Ling,†,‡ and Marie-Paule Pileni*,‡,§

†Institut Parisien de Chimie Moléculaire, Sorbonne Universités, UPMC-Univ Paris 6, UMR CNRS 8232, F-75005 Paris, France
‡MONARIS,Sorbonne Universités, UPMC-Univ Paris 6, UMR CNRS 8233, F-75005 Paris, France
§CEA/IRAMIS, CEA Saclay, 91191 Gif-Sur-Yvette, France

ABSTRACT: *N*-Heterocyclic carbenes (NHCs) have emerged as a new class of ligands for materials chemistry that appears particularly relevant for the stabilization and functionalization of metal nanoparticles (NPs). The particular properties and high synthetic flexibility of NHCs make them highly attractive tools for the development of new (nano)materials and the fundamental study of their properties. The relationships between the NHC structure and NP structure/properties, including physical, biological, and self-assembly properties, remain largely unknown. In the past decade, many efforts have been made to gain more fundamental understanding in this area. In this feature article, we present our contribution in this field focusing on the formation of NHC-coated Au nanocrystals (NCs), their stability, and their ability to self-assemble into 3D crystalline structures called supracrystals. First, the formation of NHC-stabilized Au NCs is discussed by comparing different NHC structures, NHC-based Au precursors, and synthesis methods. This study shows the major role of the NHC structure in obtaining both stable NHC-coated Au NCs and narrow size distributions. In a second part, a comparative study of the oxygen resistance of NHC- and thiol-coated NCs is presented, demonstrating the enhanced stability of NHC-coated Au NCs to oxygen-based treatments. Finally, the self-assembly of NHC-coated Au NCs into 3D Au superlattices is presented. The formation of large organized domains of several micrometers is described from the design of NHCs tailored with long alkyl chains. In these different contexts, efforts have been made to gain a more in-depth understanding of the behavior of NHC ligands at the surface of NCs. These results show that the NHC-based approach to nanomaterials has many assets for opening a new research area in the supracrystal world.
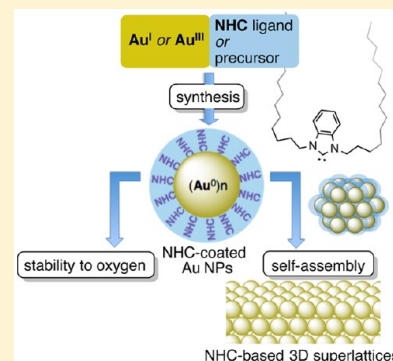
INTRODUCTION

The properties of nanomaterials are strongly connected to their ordering at the atomic scale (nanocrystallinity).[1] In ordered nanoparticles, called nanocrystals, surface coating by a ligand is often essential to bring stabilization and additional functionality to the metallic core.[2,3] The ligand also plays a major role in the synthesis process by controlling the NC shape, size, and size distribution, which are determinant factors affecting their physical properties,[4,5] their ability to self-assemble into 2D or 3D superstructures, and beyond, the generation of new materials. Hence, changing the nature of the ligand can dramatically affect the structure and properties of metal-based NCs and metallic NC-based materials.[6] This is of great interest in investigating the fundamental properties of nanomaterials to direct their properties and to develop materials associated with new functions.

Au NPs have attracted particular interest for their size-related optical, magnetic, and electronic properties[7,8] as well as for their potential applications in catalysis[9,10] and biology.[11–14] Au NPs are among the most stable metal NPs and as such have often been used as models for the development of other metal-based nanomaterials. Au NPs (and other metal NPs) can self-assemble into higher-order crystallographic structures including 3D superlattices also called supracrystals.[15–17] Many types of

surface ligands have been employed in the synthesis of Au NPs,[18] including carboxylates (citrate), phosphorus ligands, and nitrogen-based or sulfur-based ligands (e.g., alkanethiols). Functionalized thiol-coated Au NPs have been among the most widely studied because of the stabilization provided by the strong S—Au bond and the possible high packing density of thiols at the surface (Figure 1A). However, the S—Au bond is not completely inert, and the long-term stability of Au NPs and derived materials remains a major concern for the development of safe and reliable applications.[19,20] More generally, there is still an important need for alternative ligands to develop new applications of nanomaterials.

In recent years, *N*-heterocyclic carbenes (NHC, Figure 1B)[21–24] have attracted increasing attention as neutral C-ligands for nanomaterial stabilization and functionalization.[25–43] This topic was recently reviewed by Johnson and co-workers.[44] NHC-based SAMs on Au surfaces have also been reported.[45–47] NHCs present many advantages for nanomaterials. First, a wide range of NHC structures are available as a result of extensive applications in organometallic chemistry and
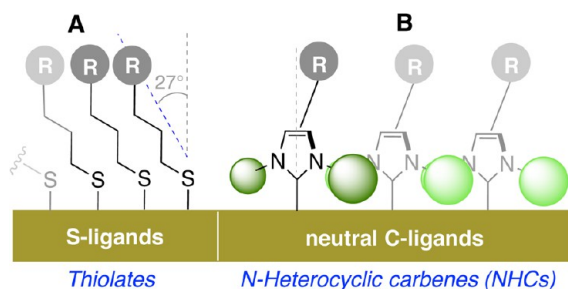
Figure 1. Simplified depiction of the structure and bonding on a metallic surface of (A) commonly used thiolate ligands and (B) neutral NHC ligands. R represents long alkyl chains or functionalized groups. The green spheres represent the substituents of the nitrogen atoms on the NHC ligands.

catalysis. The high synthesis flexibility allows for the fine-tuning of steric and electronic properties and facilitates the introduction of functional groups at different positions.[48] NHCs exhibit a particular geometry, different from that of most commonly used (linear) ligands. The N-substituents of the NHCs point out from both sides and are oriented toward the metallic surface, inducing significant interactions with the metallic surface and the neighboring ligands (Figure 1B). Therefore, NHC structure modulations can dramatically affect the NHC bonding mode, the surface coverage, and the ligand packing density as well as the number of free metallic sites available for catalysis. Finally, the strong σ-donating properties of NHCs are expected,[49] as in metal complexes,[50] to provide strong NHC−metal bonds at the surfaces. The most commonly used method for obtaining NHCs involves deprotonation of the precursor azolium salts.[48] However, in contrast to many metal−NHC complexes, free NHCs are highly sensitive to oxygen, water, and carbon dioxide and should be handled with the exclusion of air and moisture. In many experimental procedures, NHCs and metal-ligated NHCs are generated in situ under an inert atmosphere.[21−23]

Various synthesis methods have been tested for the formation of metal (M) NPs stabilized by NHC ligands (M = Ir, Ag, Au, Ru, Pd, Pt).[25−43] Since the work of Finke in 2005 suggesting surface attachment of 1-methyl-3-butyl imidazolylidene as an NHC ligand on Ir[0] nanoclusters,[25] various NHC structures have been investigated (Figure 2). The synthesis flexibility has been exploited to introduce long alkyl chains,[27,29,39−41] chiral moieties,[32] hydrosoluble chains,[37,43] and more complex polyaromatic structures.[36,38] Some NHC-based metal NPs have been applied in metal-catalyzed hydrogenation reactions (M = Ir, Ru, Pd, Pt).[26,32−34,37,39,43] The enhanced stability of NHC-based SAMs and NPs to oxidative treatments was reported very recently.[42,47]

For our part, we first examined the ability of well-defined and easily accessible NHC−Au[I] complexes bearing common NHC ligands (e.g., Et₂Bimy, IMes, and IPr in Figure 3) to generate stabilized Au NCs under reductive conditions. At that time, no indications were available on the most suitable NHC structures to be used for this purpose. This prompted us to further assess the influence of different NHC structures on the control of NC size and size distribution and on their stabilization (Figure 3).[51] Next, we sought to determine whether NHC-coated Au NCs exhibit greater resistance to oxygen-based treatment than their thiol-coated analogues,[52] which is essential information for future applications. Finally, we explored the 3D self-assembly of NHC-coated Au NCs into supracrystals that involved the
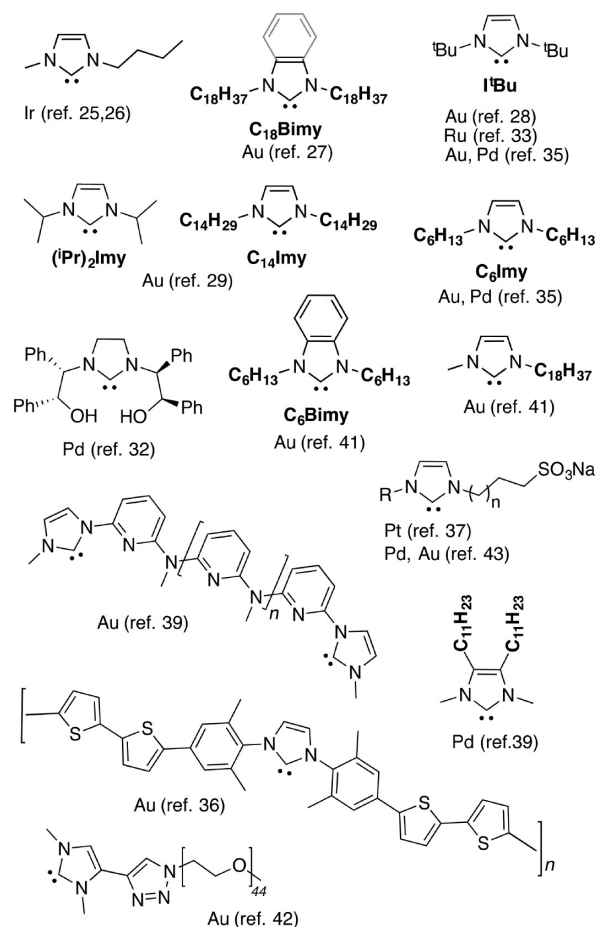

Figure 2. Selected NHC ligands reported for the stabilization and/or functionalization of metal NPs. Mes = 1,3,5-trimethylphenyl. Imy and Bimy are commonly used acronyms for imidazolylidene and benzimidazolylidene, respectively.
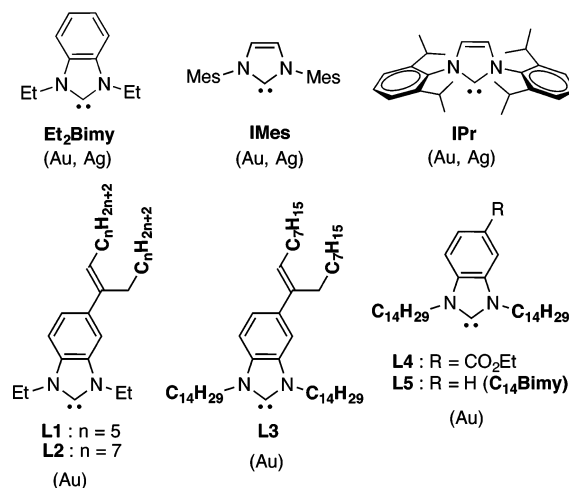
Figure 3. Representative structures of NHC ligands investigated in our studies for Au NC stabilization.[51−53] Et₂Bimy = 1,3-diethylbenzimidazolylidene, IMes = 1,3-bis(2,4,6-trimethylphenyl)imidazolylidene, and IPr = 1,3-bis(2,6-diisopropylphenyl)imidazolylidene. NHC ligands L1−L5 were designed more particularly for Au NC self-assembly into 3D Au supracrystals.

design of a series of NHC ligands with long alkyl chains at different positions (L1−L5 in Figure 3).[53] This area, which

offers the opportunity to develop new NHC-based materials with original properties, was virtually unexplored. The main results of these studies are presented herein.

■ SYNTHESIS OF AU NANOCRYSTALS FROM NHC-BASED AU[I] AND AU[III] PRECURSORS

Synthesis of Au NCs from [(NHC)AuCl] Complexes.
Controlling the size and stability of NPs is the first major challenge when new ligands are introduced in NP synthesis. By comparison with thiols, examples of NHC-coated Au NPs or NCs (or other metal NPs) associated with strong control of the size distribution (standard deviation σ < 10%) remain extremely rare.[29] To achieve this, we first explored synthesis routes to NHC-based Au NC from NHC−Au[I] complexes based on the one-phase Stucky method previously used for the preparation of thiol-coated metallic NCs.[54,55] This method was initially shown to provide Au NCs with strong control of the size and size distribution (σ < 5%) by the homogeneous reduction of triphenylphosphine gold chloride [(PPh$_3$)AuCl] in organic solvents in the presence of excess dodecanethiol (DDT, $C_{12}H_{25}SH$). Furthermore, it led to a mixture of NCs differing by their crystalline structure (single domain and polycrystals).[55] By analogy, [(NHC)AuCl] complexes have been considered to be attractive analogues of [(PPh$_3$)AuCl] for the one-phase synthesis of Au NCs. Here, the NHC can play a dual role both as a ligand for the initial Au[I] species and as a stabilizing agent for the metallic NCs formed (Figure 4). This general strategy, which does not require the preparation of free NHCs, is depicted in Figure 4.
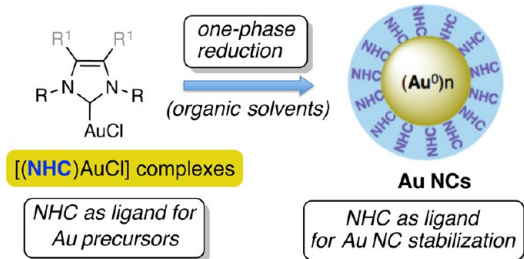

Figure 4. Strategy for synthesizing NHC-coated Au NCs by the one-phase reduction of well-defined [(NHC)AuCl] complexes.

The introduction of NHC ligands instead of PPh$_3$ is also interesting for investigating steric and electronic effects associated with the organic ligand in the process of NC formation. Modulation in the NHC structure can change the reduction rate of Au[I] or Au[III] precursors to give Au[0] NCs and thus alter the NC size and size distribution. Because of the strong σ-donor effect of the NHC ligand, metal−NHC complexes are more difficult to reduce than the corresponding phosphane-based complexes.[56] The reduction of [(IPr)AuCl] bearing the bulky NHC ligand IPr (Figure 3) was first shown in 2008 to give a stable Au[I] hydride complex [(IPr)AuH].[57] The formation of Au NPs or aggregates (both not expected in this work) was not noted. Tilley and co-workers reported for the first time in 2009 the formation of Au NCs by the reduction of NHC−Au[I] precursors bearing two different imidazole-based NHCs, (^{i}Pr)$_2$Imy and C_{14}Imy (Figure 2).[29] The formation of relatively monodisperse Au NCs (5.75 ± 0.49 nm, σ = 8.5%) was achieved by reduction with 9-BBN of [(C_{14}Imy)AuCl] bearing an NHC ligand with long alkyl chains.

To assess the effect of varied NHC structures on the formation of Au NCs, we investigated the one-phase reduction of four [(NHC)AuCl] complexes bearing Et$_2$Bimy, IMes, IPr, or **L5** as NHC ligands (Figure 5).[51]
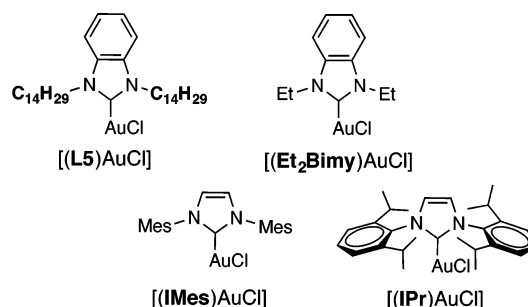

Figure 5. Well-defined [(NHC)AuCl] complexes investigated in the one-phase synthesis of Au NCs.

We initially used ammonia−borane complex (NH$_3$BH$_3$) in toluene at 100 °C as reductive conditions (method A). Different results were obtained depending on the nature of the NHC ligand initially present on the complex (Figure 6).
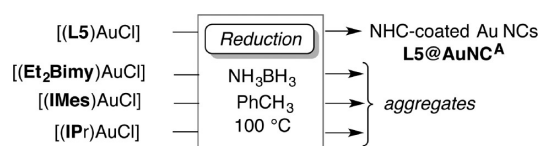

Figure 6. One-phase reduction of [(NHC)AuCl] complexes by NH$_3$BH$_3$ (method A). Large hexagonal Au NCs (**L5@AuNC**[A], 9.8 nm, σ = 6.9%) were obtained from [(**L5**)AuCl] in which the NHC ligand **L5** bears long C14 alkyl chains. The reduction of [(**Et$_2$Bimy**)-AuCl], [(**IMes**)AuCl], and [(**IPr**)AuCl] led to the precipitation of bulk Au materials.

The three complexes {[(**Et$_2$Bimy**)AuCl], [(**IMes**)AuCl], and [(**IPr**)AuCl]} led to the formation of large aggregates. The precipitation of bulk materials was consistently observed with these three complexes regardless of the various conditions tested. In contrast, the reduction of [(**L5**)AuCl] through method A was found to allow the isolation of stabilized Au NCs. (**L5@AuNC**[A]). In this case, large hexagonal NCs with an average size of 9.8 nm and a narrow size distribution (±6.9%) were obtained (Figure 7).[58] These preliminary results highlighted the great influence of the NHC structure on NC formation and stabilization. The specific feature of NHC **L5** lies in its C14 long alkyl chains on the nitrogen atoms. This suggests that the stabilization of Au NCs could be favored by NHCs with long alkyl chains such as **L5** or C_{14}Imy. However, limited long-term stability was observed for **L5@AuNC**[A], which precipitates from the toluene solution after 12 h.

The formation of aggregates from complexes [(**Et$_2$Bimy**)-AuCl], [(**IMes**)AuCl], and [(**IPr**)AuCl] suggests that NHCs **Et$_2$Bimy**, **IMes**, and **IPr**, having significantly different steric and electronic properties, do not prevent the corresponding Au[I] complexes from being reduced by hydrides to form Au[0] but more likely are inefficient to stabilize Au clusters or nanocrystals.

To limit the aggregation of Au[0], an alternative strategy was investigated where dodecanethiol (DDT) was introduced into the reaction medium prior to reducing agent addition (method B, Figure 8). This method, close to that initially reported with
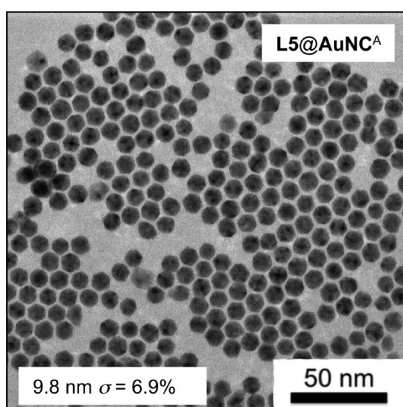
Figure 7. Transmission electron microscopy (TEM) images and size of NHC-stabilized Au NCs obtained after the reduction of [(**L5**)AuCl] by NH$_3$BH$_3$ at 100 °C in toluene (method A). Au NCs dispersed in toluene were deposited on a TEM grid covered by amorphous carbon. The average diameter (in nm) and the size distribution (standard deviation σ) were determined from the TEM images by using ImageJ software (dm3 plugin) and by measuring about 500 NCs in arbitrarily chosen areas of the photographs.
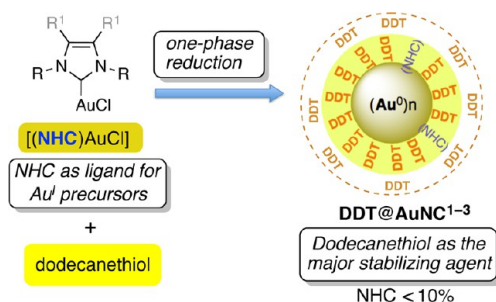

Figure 8. Preparation of Au NCs by the reduction of [(NHC)AuCl] complexes in the presence of excess dodecanethiol (method B). The as-formed NCs are mainly DDT-coated but could contain a small proportion of NHC ligands (<10%). The dashed circle represents a possible second shell of unbound thiol.

Figure 9. TEM images and size of Au NCs obtained by the reduction of [(NHC)AuCl] complexes in the presence of dodecanethiol (DDT) (method B). (A) [(**Et$_2$Bimy**)AuCl] as the precursor, (B) [(**IMes**)-AuCl] as the precursor, and (C) small Au NCs obtained from [(**IPr**)AuCl].

[(PPh$_3$)AuCl] as a precursor,[54,55] successfully led to the formation of stabilized Au NCs of 2.7–6.6 nm with narrow size distributions from [(**Et$_2$Bimy**)AuCl], [(**IMes**)AuCl], and [(**IPr**)AuCl] (Figure 9A–C). However, an analysis of the ligand shell by X-ray photoelectron spectrometry (XPS) and ^{1}H NMR spectroscopy revealed a prevalence of DDT at the surface of the as-formed NCs. XPS analyses of **DDT@AuNC^1** showed a S/N ratio of 17.7, indicating a large excess of sulfur-containing species compared to nitrogen-containing species (NHC-based molecules). A S/Au ratio of 3:1 was also measured,[59] indicating the presence of a large excess of DDT at the surface. This has been similarly observed for DDT-coated Au NCs generated by the standard Stucky procedure.[60,61] In contrast, a low N/Au ratio of 0.17:1 was determined from XPS. Assuming that the NHC ligand is the only nitrogen source, S/NHC and NHC/Au ratios of 35.4 and 0.086 are obtained, respectively. The NHC/Au ratio suggests that the maximum proportion of NHCs at the surface is less than 10%. ^{1}H NMR observations confirmed this large excess of DDT. Consequently, for **DDT@AuNC^1** the model presented in Figure 8 can be proposed, in which, because of the presence of excess thiol, a first shell of bound thiol (or thiolate) associated with a possible small proportion of NHC ligands is surrounded by a second shell of unbound thiol or disulfide.[62] The presence of a small number of NHC ligands

at the surface of **DDT@AuNC$^{1-3}$** that could be exploited for surface functionalization needs to be further demonstrated. Interestingly, **DDT@AuNC$^{1-3}$** are stable in solution in toluene for weeks. In addition, control of the NC size by the NHC ligand was observed. The bulky NHC **IPr** present on [(**IPr**)AuCl] led to small NCs (**DDT@AuNC^3**) of 2.7 nm (Figure 9C), contrasting with the NC size of ca. 6.5 nm obtained from [(**Et$_2$Bimy**)AuCl] and [(**IMes**)AuCl] (Figure 9A,B).

Synthesis of NHC-Coated Au NCs from Chloroaurate-(III) Azolium Salts. To avoid the presence of additional stabilizing agents such as DDT and obtain stable Au NCs exclusively coated by NHC ligands, we next investigated the one-pot deprotonation/reduction reaction of azolium metal-lates reported by Beer and co-workers in 2013.[35] This method is highly attractive as a convenient and economical procedure that does not require the preparation of well-defined metal–NHC complexes and in which air-sensitive NHC ligands are generated in situ and not isolated. This sequence was shown by Beer to give stabilized Au NPs from [C$_6$Imy–H][AuCl$_4$], the precursor of the C$_6$Imy NHC ligand having n-hexyl chains (Figure 2). However, large Au NPs of 16.6 nm with a relatively wide size distribution (±49%) have been obtained, showing the difficulty of controlling the NP size with this ligand.

We compared a series of benzimidazolium chloroaurate salts of general formula [(**NHC**−H) (AuCl$_4$)] (Figure 10),[53]
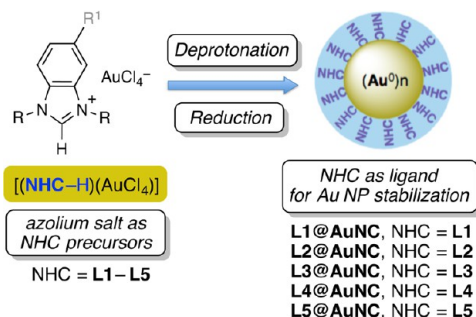

Figure 10. Preparation of NHC-coated Au NCs **L1−L5@AuNC** from benzimidazolium chloroaurate salts (method C). NHC ligands **L1−L5** functionalized by long alkyl chains have been used (Figure 3).

precursors of NHCs **L1−L5** (Figure 3), in which the heterocycle is functionalized by C7−C14 long alkyl chains. All five salts, although differing in the length and position of the alkyl chains, were found to generate stabilized Au NCs (**L1−L5@AuNC**) of 4−6 nm after treatment by NaH as the base and reduction by NaBH$_4$ at 0 °C (method C). **L1−L5@AuNC** are stable for weeks as clear purple−red colloidal solutions in toluene.

TEM analyses revealed the presence of relatively nonuniform Au NCs displaying larger size distributions than those obtained with methods A and B (from [(NHC)AuCl] complexes), ranging from 13.3 to 20.4% (Table 1). However, NCs with

Table 1. Summary of NHC-Coated Au NC L1−L5@AuNC Properties: Average Diameter (d) and Size Distribution (Standard Deviation, σ)

	before size selection		after size selection	
Au NCs	d (nm)	σ (%)	d (nm)	σ (%)
L1@AuNC	5.9	13.3	6.0	9.2
L2@AuNC	5.7	20.4	5.7	11.2
L3@AuNC	3.5	19.9	4.0	11.9
L4@AuNC	5.4	16.4	5.2	10.2
L5@AuNC	4.7	15.5	5.0	10.1

narrower size distributions of 9−12% could successfully be obtained by centrifuging at different speeds (Table 1). This procedure does not change the average size that remains similar to that observed before selection. This size selection was particularly important for studying the self-assembly of the NCs, which is addressed in a later section. A detailed procedure for the synthesis of **L1−L5@AuNC** and size selection is shown in Figure 11.

The presence of the NHC ligands as stabilizing agents at the surface of **L1−L5@AuNC** was demonstrated by ¹H NMR and XPS. The ¹H NMR spectrum of **L5@AuNC** showed the presence of NHC-based species with typical signal patterns and chemical shifts corresponding to the benzimidazole moiety. These signals are very similar to those of the well-defined [(**L5**)AuCl] complex used as a reference, suggesting that in situ-generated NHCs are transferred to the surface of the NC Au core. An important broadening of some signals of the long alkyl chains, characteristic of ligands bound at the surface of NCs, is also observed. Furthermore, no trace of chloride is visible by XPS, ruling out a possible stabilization of Au NCs by
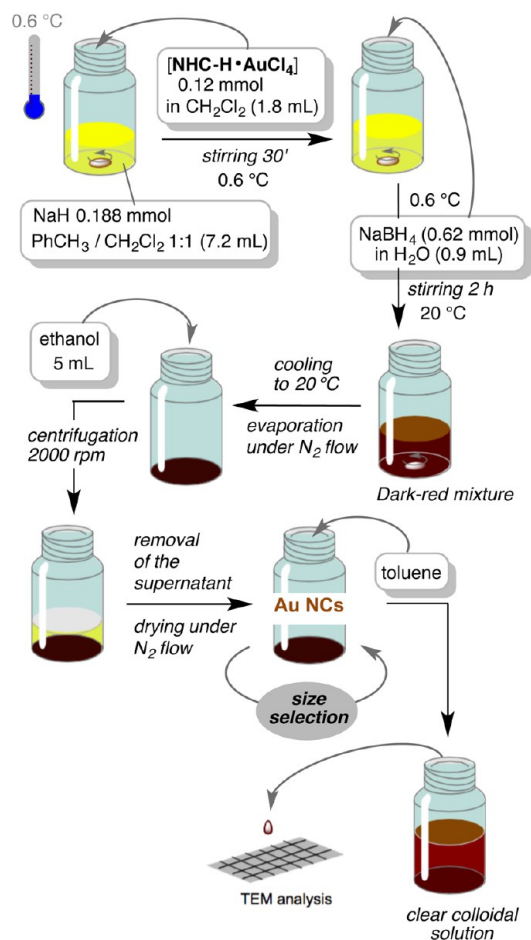
Figure 11. Typical procedure (method C) for the preparation of NHC-coated Au NCs **L1−L5@AuNC** from benzimidazolium chloroaurate salts (in a glovebox). Size selection: a colloidal solution of Au NCs in toluene (4 mL) was centrifuged at 15 000 rpm for 30 min. The supernatant was removed, and the residual precipitate was dissolved in toluene (2 mL). The mixture was centrifuged at 13 000 rpm for 30 min to give in the supernatant NHC-coated Au NCs with improved size distribution.

an azolium chloride salt. The XPS data showed the presence of nitrogen, with a N 1s signal having a binding energy of 401 eV, similar to that of the well-defined [(**L5**)AuCl] complex, also supporting the presence of the NHC ligand (having two nitrogen atoms) at the surface of the NCs. In addition, the Au 4f signal of **L5@AuNC** showed a predominant Au species, having binding energies (88.0 and 84.0 eV) consistent with those of bulk metallic Au⁰.[63−65] A N/Au ratio of 1:4.4 was determined for **L5@AuNC**, corresponding to a NHC/Au ratio of ca. 1:9. Considering that each **L5** NHC ligand bears two long alkyl chains, this corresponds to a relatively high packing of the NHC ligands at the surface of the NCs.

Different NC sizes of 4, 5, and 6 nm have been obtained with ligands **L1−L5**. TEM images of **L1**, **L3**, and **L5**-based Au NCs are shown in Figure 12. The difference in NC size was ascribed to the different volumes of the NHC ligands. Larger particles of ca. 6 nm are obtained with **L1** and **L2** characterized by small ethyl groups on the nitrogen atoms whereas the most bulky NHC **L3** gives the smallest particles of 4 nm. This trend was consistently observed with different batches. This is consistent with previous studies showing that bulky thiol ligands resulted in smaller core sizes by comparison with nonbulky ligands.[66] It

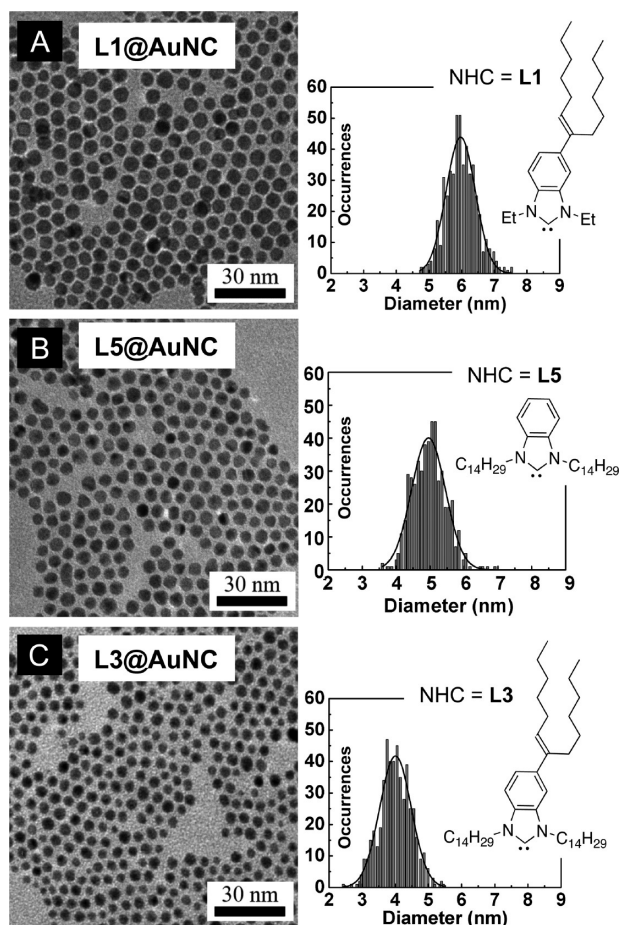**Figure 12.** Selected TEM images and size distributions of NHC-coated Au NCs obtained by the deprotonation/reduction reaction of the corresponding chloroaurate benzimidazolium salts [(**L1**−H)-(AuCl$_4$)] (A), [(**L5**−H)(AuCl$_4$)] (B), and [(**L3**−H)(AuCl$_4$)] (C) after size selection.

Figure 13. Three-dimensional representations of **L1** (A), **L5** (B), and **L3** (C) on a gold surface comparing the relative sizes of the NHC ligands. Three-dimensional models were built with Avogadro and minimized with UFF (universal force field).

is likely that the C14 alkyl chains of **L3**−**L5** increase the volume of the NHC ligand close to the surface of the metallic core. This is particularly significant for **L3** in which the intramolecular steric interactions between the long alkyl chains may lead to the largest ligand size (Figure 13).

■ STABILITY OF NHC-COATED GOLD NANOCRYSTALS TO OXYGEN-BASED TREATMENTS

The oxygen stability of Au nanomaterials is a major issue for the development of devices that will be exposed to air or for in vivo applications where they can be exposed to radical oxygen species.[20] In both cases, the integrity of the nanomaterials must be controllable to achieve reliable results. NHC ligands have emerged as promising tools to improve the stability of Au-based nanomaterials to oxidative treatments. Recently, NHC-based SAMs and NHC-PEG conjugates were both shown to provide high resistance to hydrogen peroxide treatments to Au(111) surfaces and Au NCs, respectively.[42,47]

In our study, we sought to compare through TEM, NMR, and UV analyses the effects of pure oxygen and of oxygen plasma treatment (containing radical oxygen species) on NHC-based and thiol-based Au NCs.[67] Different batches of DDT-coated Au NCs, prepared by different routes, and of NHC-
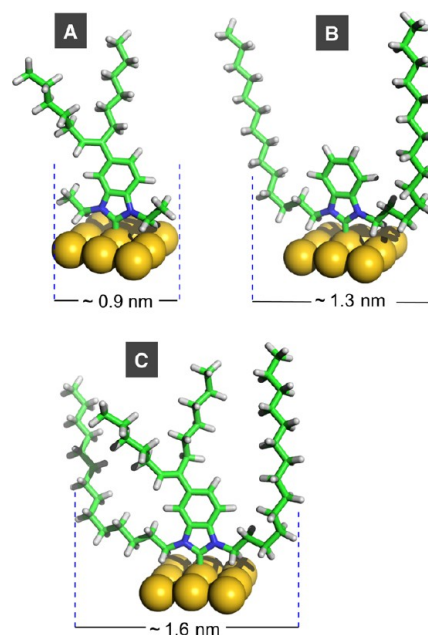
coated Au NCs bearing different NHC ligands, have been examined in parallel.

Resistance of NHC-Coated and DDT-Coated Au NCs to Oxygen Plasma Treatment. Oxygen plasma exposure at different times was used to compare the stability of **DDT@AuNC$^{1−3}$**, which are DDT-coated Au NCs (with potentially a small proportion of NHC ligands), with that of **L1−L5@AuNC**, which are NCs coated exclusively by NHCs. In addition, two series of DDT-coated Au NCs were prepared from [(PPh$_3$)AuCl] as the precursor (**DDT@AuNC^4**)[54] or through reverse micelles from AuCl$_4^−$ (**DDT@AuNC^5**)[68] to exclude the presence of NHCs at the surface of DDT-coated NCs. Before exposure, all Au NCs were dispersed in toluene and analyzed by TEM to obtain a reference image corresponding to the sample without exposure to oxygen (i.e., $t_{exposure}$ = 0 s). By using numbered carbon-covered copper grids, we recorded TEM images of the same area of the samples after exposure.

Before exposure, all NCs appear as ordered hexagonally arranged 2D networks in which the NCs are well-separated (selected TEM images shown in Figure 14A−D). All samples were subjected to oxygen plasma at increasing exposure times from 60 to 120 s to assess their resistance to the treatment. From an exposure time of 80 s, we could clearly differentiate the resistance of DDT and NHC-coated Au NCs. These conditions generate a large proportion of coalesced objects from all DDT-coated Au NCs (**DDT@AuNC$^{1−5}$**), whereas no change in NC integrity is observed for NHC-coated Au NCs. The alteration of **DDT@AuNC^1** and **DDT@AuNC^3** after 80 s of treatment is shown in Figure 14E,F. A dramatic change in the monolayer can be observed in the TEM images where many adjacent Au NCs are bound together and form ill-defined objects resulting from coalescence. The oxidative treatment at 80 s affects all of the DDT-coated Au NCs, regardless of the synthesis method or precursor used for the synthesis. In addition, their sensitivity against aggregation, when arranged

Figure 14. TEM images of DDT-coated (left) and NHC-coated (right) Au NCs deposited on an amorphous carbon-covered TEM grid before oxygen plasma exposure (t = 0 s): (A) **DDT@AuNC[1]** generated from [(Et$_2$Bimy)AuCl], (B) **DDT@AuNC[4]** generated from [(PPh$_3$)AuCl], (C) **L3@AuNC** (NHC = **L3**), and (D) **L4@AuNC** (NHC = **L4**). The same areas after exposure to oxygen plasma for 80 s at 10 W [(E) **DDT@AuNC[1]** and (F) **DDT@AuNC[4]**] or 120 s at 10 W [(G) **L3@AuNC** and (H) **L4@AuNC**]. Numbered carbon-covered copper grids were used to identify the areas before and after exposure. The TEM grids with the NC samples were loaded into the RIE apparatus (reactive ion system Plassys MG 200). The plasma treatment was carried out using oxygen as the etching gas, with a working pressure maintained at 4 μbar and an oxygen flow rate of 10 sccm. The experiments were repeated twice.

into 2D networks, seems to be independent of NC size as indicated by the similar resistance of **DDT@AuNC[3]** (2.7 nm) and other DDT-coated Au NCs (6.2−6.9 nm) (data not shown).[52]

All NHC-based Au NCs (**L1−L5@AuNC**) were found to be resistant to oxygen plasma treatment for an increased exposure time of 120 s. The TEM images at 120 s revealed that the NCs remained structurally unaffected by the treatment. No change in either the NCs integrity or their 2D assembly is detectable as shown for **L3@AuNC** and **L4@AuNC** (Figure 14G,H). Subsequently, **L5@AuNC** was used as a sample to test an extended exposure time of 180 s. Here again, both the integrity and the 2D arrangement of **L5@AuNC** NCs were found to remain unchanged after treatment (Figure 15). This experiment could not be reproduced with the same quality on other samples because of the degradation of the carbon film on copper grids induced by long-time exposure (the film is totally broken down at an exposure time exceeding 180 s). However, these results suffice to demonstrate that NHC-coated Au NCs exhibit a remarkable and enhanced resistance to oxygen plasma by comparison with DDT-coated Au NCs. This is consistent with the relative Au−ligand bond strengths. Higher bond dissociation energies (BDE) have been reported for the C$_{carbene}$−Au bond on Au(111) surfaces by comparison with typical S−Au bonds on Au surfaces.[46,47,69,70] This should follow the same trend with Au NCs, providing higher oxygen stability to the NHC−Au unit and thus higher stabilization of NHC-coated NCs. The exact phenomenon involved in the degradation or modification of NCs after treatment with

Figure 15. TEM images of **L5@AuNC**: (A) before oxygen plasma exposure (t = 0 s); (B) the same area after exposure to oxygen plasma for 180 s at 10 W.

oxygen plasma remains to be determined. After exposure, the NCs are difficult to redisperse from the TEM grids, and the amounts of matter deposited on the grids are too low for further characterization.

Influence of Molecular Oxygen on the Stability of NHC- and DDT-Coated Au NCs. To further assess the stability of NHC-protected Au nanocrystals and compare with that of thiol-based NCs, additional experiments were implemented where solid samples of NHC-stabilized Au NCs **L5@AuNC** and DDT-coated NCs **DDT@AuNC[4]** were exposed to molecular oxygen (O_2) for 1 week at room temperature. ^{1}H NMR, UV−vis, and mass spectroscopy were used to analyze the colloidal solutions of the samples before and after exposure to oxygen. Control experiments were also carried out where the dried solid samples of the same NHC-based Au NCs (**L5@AuNC**) and DDT-coated NCs (**DDT@AuNC[4]**) were exposed to nitrogen (N_2) for 1 week. For an accurate analysis of NC concentrations, UV−vis spectra were recorded in toluene before and after O_2 exposure (Figure 16).
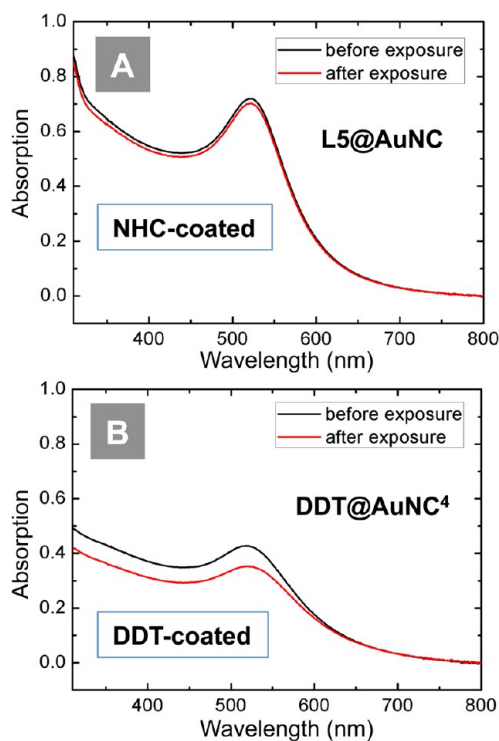

Figure 16. UV−vis spectra of **L5@AuNC** (A) and **DDT@AuNC[4]** (B) before and after 1 week of exposure to O_2 (1 atm) at 20 °C. A suspension of 1 mg of Au NCs in toluene (1 mL) was prepared and then diluted 20-fold for the analysis.

For NHC-coated **L5@AuNC**, the comparison of the spectra shows that the concentration of NCs in the colloidal solution after exposure to O_2 has slightly decreased by 2.5% (Figure 16A). In contrast, the UV−vis spectra of a suspension of **DDT@AuNC[4]** before and after 1 week of exposure to oxygen show a significant difference in absorption corresponding to an important decrease in Au NC concentration of about 17.5% after exposure (Figure 16B). In the control experiments carried out under N_2 for 1 week, no difference could be detected in the UV−vis spectra of **L5@AuNC** and **DDT@AuNC[4]** before and after exposure, thus demonstrating that both DDT-coated and NHC-coated NCs remain stable under these conditions (data

not shown).[52] Therefore, these results demonstrate that the integrity of DDT-coated Au NCs is more affected by O_2 treatment than that of their NHC-coated analogues. The partial degradation of DDT-coated **DDT@AuNC[4]** after exposure to O_2 was visible to the naked eye in NC dispersion in toluene where a precipitate is visible. In addition, the solution exhibits a lighter color than the solution of the sample before exposure having the same initial mass concentration. In contrast, no visible changes were detected in colloidal solutions of NHC-coated **L5@AuNC** before and after exposure to O_2, which both occur as deeply colored mixtures with no visible precipitate. ^{1}H NMR spectroscopy was used to investigate the chemical processes involved in NC degradation under O_2 treatment. The initial samples of **L5@AuNC** (coated with NHC **L5**) and **DDT@AuNC[4]** (coated with DDT) were dissolved in CD_2Cl_2 (0.6 mL) and analyzed by ^{1}H NMR before O_2 exposure. Then the same samples were transferred in a setup in which the oxygen atmosphere was introduced through vacuum/O_2 cycles. The as-obtained dry samples were kept under a light flow of O_2 for 1 week. After exposure, the sample were redispersed in CD_2Cl_2 (0.6 mL) and directly analyzed by ^{1}H NMR spectroscopy.

For **L5@AuNC**, the ^{1}H NMR spectrum of the sample after treatment was found to be very similar to that of the initial sample. It shows a major species corresponding to the bound NHC ligand as observed before oxygen exposure.[52] However, a new set of signals that was attributed to an NHC-derived molecule was also visible in the spectrum. On the basis of the integration of the NMR signals, we assumed that about 15−20% of the bound NHC ligand was converted to this new species, which corresponds neither to the azolium chloroaurate or chloride salts nor to the [(NHC)AuCl] complex. Consequently, although no precipitation of bulk materials is observed after O_2 treatment of NHC-coated Au NCs, indicating high stability, it seems that the surface NHC ligands may still be partially modified during treatment. After 1 week of N_2 treatment, used as a control experiment, no significant changes are detected in the NMR spectrum of the colloidal solution, confirming that the modification is O_2-induced. For DDT-stabilized **DDT@AuNC[4]**, we showed that the initial sample before O_2 exposure contains a significant amount of free ligands (DDT and traces of disulfide) as previously observed by XPS. From the NMR spectrum, the ratio of bound DDT to free ligands was estimated to be 1:1.[71] This is consistent with the NC structure previously proposed in Figure 8. After oxygen treatment, the major difference observed is a significant increase (~15%) in the amount of free disulfide, indicating that about 30% of DDT is oxidized.[72] On the basis of the integrations of the NMR signals, the proportion of bound DDT was estimated to be 35% of all DDT-based species present in the solution. Free DDT is still largely present at a percentage of 35%. In the control experiment carried out under nitrogen, no significant difference is observed before and after treatment. Therefore, the oxidation of DDT under O_2 treatment seems to be a major phenomenon leading to the partial degradation of DDT-coated NCs and to the precipitation of bulk materials, as observed in the colloidal solution. Next, we sought to determine whether a particular species can be formed during the oxygen treatment of NHC-coated Au NCs and released in the medium after the formation of the colloidal solution. To achieve this, a sample of **L5@AuNC** previously exposed to O_2 for 1 week was dispersed in toluene, and the NCs were precipitated by the addition of methanol followed by centrifugation. The residual supernatant

was analyzed by mass spectroscopy. Interestingly, the spectrum revealed the presence of a major positive ion with m/z = 1217.9640 that was unambiguously ascribed to the cationic $[(NHC)_2Au]^+$ complex. Prior to exposure to oxygen, the mass spectrum of the supernant showed the presence of $[L5-H]^+$ (m/z = 511.4545) as the major positive ion with only traces of the bis-carbene $[(NHC)_2Au]^+$ complex. The formation of $[(NHC)_2Au]^+$ complexes from NHC-coated Au NPs and the spontaneous leaching (without oxidative treatment) of NHC–Au^I species and of free NHCs associated with nanoparticles degradation were previously reported with other NHC ligands.[28,40] It was suggested that the bis-carbene $[(NHC)_2Au]^+$ complex may form during the course of NP formation by reaction of the free NHCs with the metallic surface of Au NPs.[40] Here we show that exposure to O_2 likely induces the formation of $[(NHC)_2Au]^+$ complexes. Further studies are required to determine whether these NHC-based species formed under oxidative treatment remain bound to the surface of Au NCs and favor stabilization. Taken together, these results show that the nature of the ligand (i.e., NHC or thiol) is a major factor governing the stability of NCs. Although the bound NHC ligands at the surface of NCs are not completely insensitive to the effect of O_2, the corresponding NHC-coated Au NCs clearly show greater resistance to molecular oxygen than their thiol-coated analogues.

■ THREE-DIMENSIONAL SELF-ASSEMBLY OF NHC-COATED GOLD NANOCRYSTALS

The ordering of NCs in 3D crystalline structures, called supracrystals, has attracted particular attention for their original collective properties (electronic, magnetic, and optical) that are neither those of the isolated NCs nor those of the same material in the bulk phase. Such collective properties, due to the NC assemblies in 3D superlattices, open a new research area for creating novel materials that are potentially useful for new devices.[15,16,73] Therefore, controlling the assembly of supra-crystals and thus their properties is an important challenge for the design of new materials in which the ligands of the NC building blocks play a major role. A prerequisite for producing supracrystals is control of the NC size distribution.[74] As a consequence, predominantly Au NCs with alkanethiols as ligands but also, to a lesser extent, alkylamines and carboxylic acids have been used to grow Au superlattices.[15–17] Only one report described the formation of an NHC-based 3D-organized Au NC superstructure (NHC = C_{14}Imy) resulting from the superposition of three layers of relatively monodisperse Au NCs (5.75 nm ±8.5%).[29] This prompted us to investigate the self-assembly of our series of NHC-coated Au NCs L1−L5@ AuNC for developing new generations of structured Au supracrystals. Ligands L1−L5 (Figures 3) were specially designed to test different NHC structures, mainly differing in the length and position/orientation of the long alkyl chains on the NHC backbone. As previously presented, L1−L5@AuNC are characterized by a size distribution (σ = 9−12%) low enough to produce supracrystals (Table 1).

The controlled evaporation of colloidal solutions of thiol-based Au NCs was previously shown to give straightforward access to highly ordered and large-domain supracrystalline Au structures on solid surfaces.[15–17,75] This method was investigated for the preparation of NHC-based supracrystals from NHC-stabilized L1−L5@AuNC. Thus, colloidal dispersions of L1−L5@AuNC in toluene were introduced into a beaker, in the bottom of which was a silicon wafer, and the

solvent was slowly evaporated under N_2 at 50 °C. The as-formed films were analyzed by SEM (scanning electron microscopy). Dramatic differences in the film morphology were observed depending on the NHC ligand (L1−L5) involved in Au NC stabilization. For instance, L1@AuNC and L2@AuNC lead to films with a discontinuous top layer exhibiting small organized domains that are lying on an amorphous Au NC film. In contrast, L4@AuNC and L5@ AuNC lead to large and thick highly organized domains of several micrometers as shown in Figure 17. These results
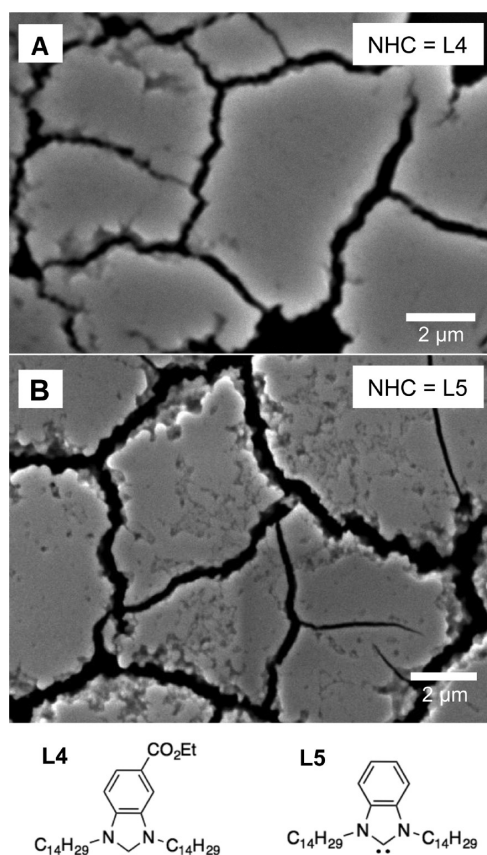

Figure 17. Scanning electron microscopy (SEM) images of L4-based (A) and L5-based (B) Au supracrystalline films of micrometer scale obtained by slow evaporation of a toluene suspension of the corresponding Au NCs (L4@AuNC and L5@AuNC) at 50 °C. The film thickness is ca. 1 μm.

demonstrate the great importance of the NHC structure for the self-assembly of NHC-based Au NCs. The structures of L4 and L5 correspond to the same design where the long alkyl chains (C_{14}) are positioned on the nitrogen atoms of the NHC (Figure 3). The success of this family of ligands in generating supracrystals is unexpected. To obtain organized 3D super-structures, the long alkyl chains of the ligands should be involved in attractive interdigitation phenomena to counter-balance the repulsive interactions between the NCs. In L4 and L5, because of the geometry of the ligand, the alkyl chains point initially in the direction of the metallic core, which does not correspond to the best orientation for inducing such stabilizing interactions. The highly organized structure of the supracrystals obtained with L5 was confirmed by high-resolution SEM (HRSEM) and fast Fourier transform (FFT) showing a well-defined hexagonal pattern (Figure 18). In addition, small-angle
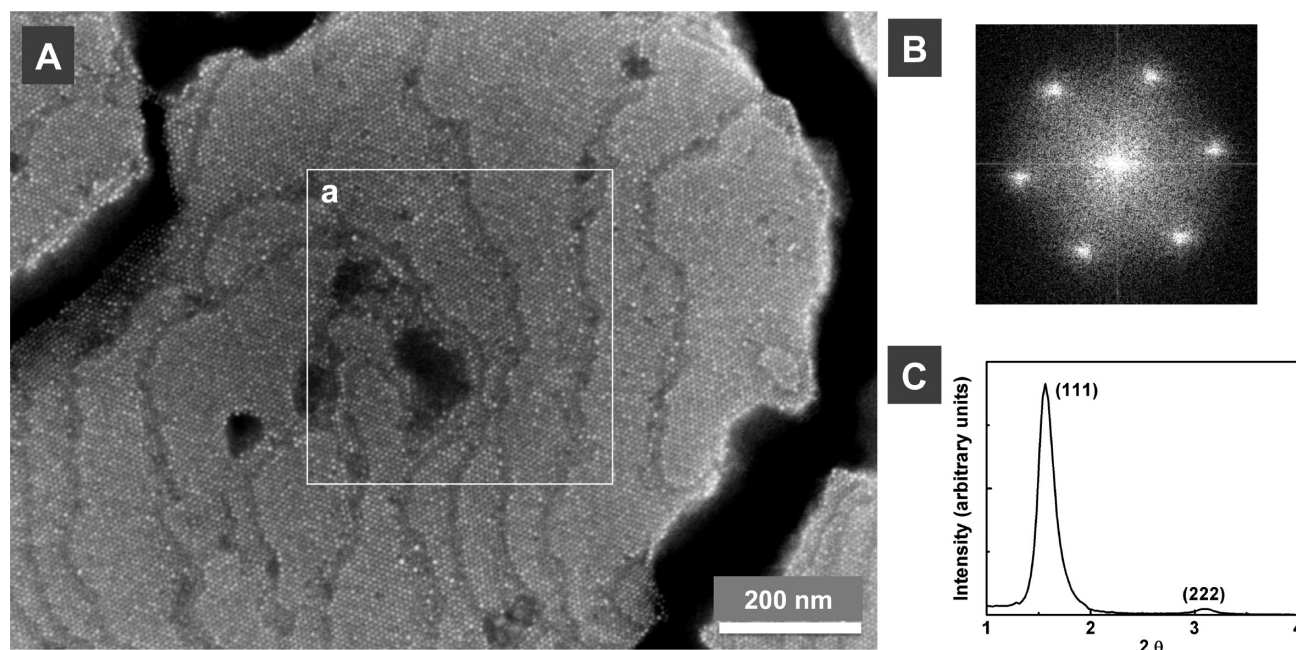
Figure 18. NHC-based supracrystal of Au NCs coated with ligand **L5**: (A) HRSEM image, (B) FFT of zone a, and (C) SAXRD pattern.

X-ray diffraction (SAXRD) analyses confirmed the formation of fcc (face-centered cubic) supracrystals with NHC ligand **L5** (Figure 18C) but also with **L4** and to a lesser extent with **L2** (small domains). The edge-to-edge distances in **L4**- and **L5**-based supracrystals were determined from the main peak of the SAXRD patterns (**L4**, δ = 1.84 nm; **L5**, δ = 2.04 nm). From all of these data, a model was proposed for **L5**-based supracrystals in which gauche defects in the alkyl chains on the nitrogen atoms enable the chains to point outward with the appropriate geometry, leading to stabilizing interdigitation phenomena in the supracrystal (Figure 19).
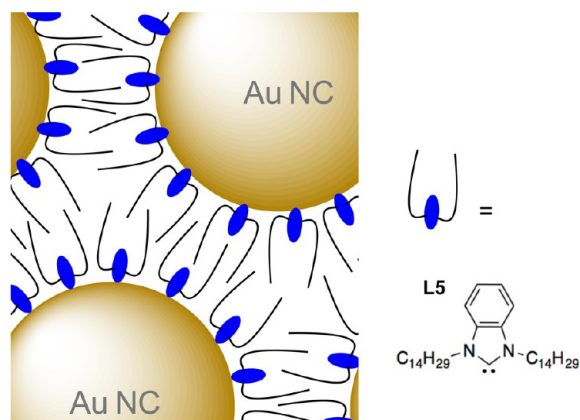

Figure 19. Proposed model for the self-assembled NHC-based supracrystals with **L5** as a ligand showing stabilizing interdigitations of the long C14 alkyl chains (in black).

CONCLUSIONS AND PERSPECTIVES

Introducing a new family of ligands in surface chemistry represents an important opportunity to develop (nano)-materials with new and original properties. In particular, ligands able to strongly bind the surface are of great interest in achieving safer and more reliable applications. Ligands of

high synthetic flexibility are also attractive for the convenient introduction of various functions and the modulation of the properties for targeted applications. Because both of these characteristics are present in *N*-heterocyclic carbenes (NHCs), these ligands have attracted increasing interest in surface chemistry. One of the main challenges in generating NHC-based supracrystals has been to control the NC size and size distribution and thus to master NC synthesis. Examples of NHC-coated metal NCs associated with strong control of the size distribution are still rare. By evaluating different NHCs, we demonstrated that the structure of the NHC ligand affected both the NC size and size distribution as well as their ability to self-assemble into organized 3D superstructures. NHCs bearing long alkyl chains led to the best results.

The production of thick and well-defined fcc supracrystals by using NHC-based NC building blocks, presented here, opens a new research area in the creation of novel materials. NHC-coated **L1−L5@AuNC** exhibit high oxygen stability compared to that of NCs coated with DDT. This can be ascribed to the greater strength of the NHC−metal bond. However, the exact nature of the stabilizing effect of NHCs on Au NCs should be further investigated. In particular, from a molecular point of view, the exact nature of NHC binding before and after oxygen treatments remains to be clarified. Interestingly, we know that DDT-based supracrystals are stable superstructures even though the corresponding discrete DDT-coated NCs are not very stable. This is due to stabilizing interdigitation phenomena and permits us to assume that the NHC-based supracrystals presented here should be very stable. This has to be confirmed and is one of the most important features of this new material. Furthermore, we need to know whether it is possible to produce other types of supracrystals by using NHC-based NCs. According to what we already produced with other hydro-phobic NCs, various opportunities are now open, taking into account the fact that NHC derivatives can be biocompatible. As recently shown in our group, such hydrophobic supracrystals could be solubilized in aqueous solution either by using phospholipids to suspend them in solution[76] or by producing

water-soluble supracrystalline colloidal eggs with free-standing 3D supracrystals.[77] We know that supracrystals are characterized by collective properties that are neither those of the isolated NCs nor those of the same material in the bulk phase.[78,79] In the future, we need to identify collective properties that could be used in various areas such as biomedicine and energy storage to build up new devices. The mechanical and optical properties of such assemblies are, in our opinion, the first needs. For the mechanical properties, according to previous observations in our group,[80] we expect to observe a drastic variation in the absolute value of Young's modulus in NHC-based supracrystals. This property was shown to be related to the interparticle distance. The interparticle distance in **L4**- and **L5**-based supracrystals varies from 1.84 to 2.04 nm, respectively.[53] Therefore, we could assume that we would produce very stable and well-defined supracrystals associated with varied mechanical properties by using different NHC ligands. Concerning the optical properties, we need to know if such localized surface plasmon resonance, LSPR, is slightly red-shifted as observed previously for thin supracrystals[81] or if new optical properties would emerge with the appearance of metamaterial properties.[82−85] According to preliminary data obtained in our group, we could expect to observe new optical properties.[86] The next properties that could be very easily explored in the next few years are related to the effect of the intrinsic crystalline structure of the NC, called nanocrystallinity, on the self-assemblies. Very recent data indicate that the crystalline structure of supracrystals and their mechanical properties are markedly affected by changes in the nanocrystallinity of the NC building blocks.[87] Taking into account all of these comments, we claim that this new NHC-based approach has many assets in opening a new research area in the supracrystal world.

■ AUTHOR INFORMATION

Corresponding Authors
*E-mail: sylvain.roland@upmc.fr.
*E-mail: mppileni@orange.fr.

Notes
The authors declare no competing financial interest.

Biographies

Sylvain Roland is an associate professor at the University P&M Curie in the Institut Parisien de Chimie Moléculaire (IPCM). He holds an M.S. in organic and bioorganic chemistry (1991) and received his Ph.D. (University P&M Curie, 1995) under the direction of J.-P. Genêt at the Ecole Nationale Supérieure de Chimie de Paris. He worked from 1995 to 1996 as a postdoctoral associate in W. B. Motherwell's group at University College London. His current research interests are in the area of metal−NHC complexes with recent applications in the biomedical field (antibiotics and anticancer agents), in nanomaterials (Au nanoparticle stabilization and self-assembly), and in homogeneous catalysis (cyclodextrin−NHC hybrid ligands for selective metal-catalyzed reactions).

Xiang Ling received his M.S. in organic chemistry from East China University of Science and Technology under the guidance of Pr. Qianfu Luo. He obtained his Ph.D. in physical and analytical chemistry from the University P&M Curie in Paris in 2015 under the direction of M.-P. Pileni and S. Roland. His research interests are organic synthesis and nanomaterials, with a particular emphasis on the design of *N*-heterocyclic carbenes as coating agents for gold nanoparticles.

Marie-Paule Pileni is a distinguished professor at University P&M Curie and a senior researcher at the Nuclear and Environmental Center, France. She is a member (1999 to present) and Chair (2004−2010) of Institut Universitaire de France, IUF, which favors the development of high-quality research and interdisciplinary projects among French universities. She has published more than 450 articles with 18 975 citations, 52.27 average citations per item and an *h* factor of 71. Prof. Pileni's research has been highly interdisciplinary over her entire scientific career, starting from biophysics to solar energy and developing nanoreactors to reach nanostructures. Her recent major breakthroughs are related to the chemical and physical properties of nanocrystals differing by their crystalline structures and/or self-assembled in 3D superlattices.

■ ACKNOWLEDGMENTS

■ REFERENCES

(1) Pileni, M.-P. Supra and Nano Crystallinity: Specific Properties Related to Crystal Growth Mechanisms and Nanocrystallinity. *Acc. Chem. Res.* **2012**, *45*, 1965−1972.

(2) Ling, D.; Hackett, M. J.; Hyeon, T. Surface Ligands in Synthesis, Modification, Assembly and Biomedical Applications of Nanoparticles. *Nano Today* **2014**, *9*, 457−477.

(3) Sperling, R. A.; Parak, W. J. Surface Modification, Functionalization and Bioconjugation of Colloidal Inorganic Nanoparticles. *Philos. Trans. R. Soc., A* **2010**, *368*, 1333−1383.

(4) Burda, C.; Chen, X.; Narayanan, R.; El-Sayed, M. A. Chemistry and Properties of Nanocrystals of Different Shapes. *Chem. Rev.* **2005**, *105*, 1025−1102.

(5) Eustis, S.; El-Sayed, M. A. Why Gold Nanoparticles Are More Precious than Pretty Gold: Noble Metal Surface Plasmon Resonance and its Enhancement of the Radiative and Nonradiative Properties of Nanocrystals of Different Shapes. *Chem. Soc. Rev.* **2006**, *35*, 209−217.

(6) Pileni, M.-P. Inorganic Nanocrystals Self Ordered in 2D Superlattices: How Versatile are the Physical and Chemical Properties. *Phys. Chem. Chem. Phys.* **2010**, *12*, 11821−11835.

(7) Sardar, R.; Funston, A. M.; Mulvaney, P.; Murray, R. W. Gold Nanoparticles: Past, Present, and Future. *Langmuir* **2009**, *25*, 13840−13851.

(8) Guo, S.; Wang, E. Synthesis and Electrochemical Applications of Gold Nanoparticles. *Anal. Chim. Acta* **2007**, *598*, 181−192.

(9) Chen, M. S.; Goodman, D. W. Catalytically Active Gold: From Nanoparticles to Ultrathin Films. *Acc. Chem. Res.* **2006**, *39*, 739−746.

(10) Hashmi, A. S. K.; Hutchings, G. J. Gold Catalysis. *Angew. Chem., Int. Ed.* **2006**, *45*, 7896−7936.

(11) Saha, K.; Agasti, S. S.; Kim, C.; Li, X. N.; Rotello, V. M. Gold Nanoparticles in Chemical and Biological Sensing. *Chem. Rev.* **2012**, *112*, 2739−2779.

(12) Boisselier, E.; Astruc, D. Gold Nanoparticles in Nanomedicine: Preparations, Imaging, Diagnostics, Therapies and Toxicity. *Chem. Soc. Rev.* **2009**, *38*, 1759−1782.

(13) Sperling, R. A.; Rivera Gil, P.; Zhang, F.; Zanella, M.; Parak, W. J. Biological Applications of Gold Nanoparticles. *Chem. Soc. Rev.* **2008**, *37*, 1896−1908.

(14) Jain, P. K.; El-Sayed, I. H.; El-Sayed, M. A. Au Nanoparticles Target Cancer. *Nano Today* **2007**, *2*, 18−29.

(15) Prasad, B. L. V.; Sorensen, C. M.; Klabunde, K. J. Gold Nanoparticle Superlattices. *Chem. Soc. Rev.* **2008**, *37*, 1871−1883.

(16) Pileni, M.-P. Self-Assembly of Inorganic Nanocrystals: Fabrication and Collective Intrinsic Properties. *Acc. Chem. Res.* **2007**, *40*, 685−693.

(17) Xu, L.; Ma, W.; Wang, L.; Xu, C.; Kuang, H.; Kotov, N. A. Nanoparticle Assemblies: Dimensional Transformation of Nanomaterials and Scalability. *Chem. Soc. Rev.* **2013**, *42*, 3114−3126.

(18) Zhao, P.; Li, N.; Astruc, D. State of the Art in the Synthesis of Gold Nanoparticles. *Coord. Chem. Rev.* **2013**, *257*, 638−665.

(19) Recent studies have shown that the thiol−Au covalent bond, which is generally considered to be relatively strong, is subject to cleavage when exposed to air, high salt concentration, elevated temperatures, or high pH. For example, see Bhatt, N.; Huang, P.-J. J.; Dave, N.; Liu, J. Dissociation and Degradation of Thiol-Modified DNA on Gold Nanoparticles in Aqueous and Organic Solvents. *Langmuir* **2011**, *27*, 6132−6137.

(20) Srisombat, L.; Jamison, A. C.; Lee, T. R. Stability: A Key Issue for Self-Assembled Monolayers on Gold as Thin-Film Coatings and Nanoparticle Protectants. *Colloids Surf., A* **2011**, *390*, 1−19.

(21) Bourissou, D.; Guerret, O.; Gabbai, F. P.; Bertrand, G. Stable Carbenes. *Chem. Rev.* **2000**, *100*, 39−92.

(22) Herrmann, W. A. *N*-Heterocyclic Carbenes: A New Concept in Organometallic Catalysis. *Angew. Chem., Int. Ed.* **2002**, *41*, 1290−1309.

(23) Hahn, F. E.; Jahnke, M. C. Heterocyclic Carbenes: Synthesis and Coordination Chemistry. *Angew. Chem., Int. Ed.* **2008**, *47*, 3122−3172.

(24) Hopkinson, M. N.; Richter, C.; Schedler, M.; Glorius, F. An Overview of *N*-Heterocyclic Carbenes. *Nature* **2014**, *510*, 485−496.

(25) Ott, L. S.; Cline, M. L.; Deetlefs, M.; Seddon, K. R.; Finke, R. G. Nanoclusters in Ionic Liquids: Evidence for *N*-Heterocyclic Carbene Formation from Imidazolium-Based Ionic Liquids Detected by ^{2}H NMR. *J. Am. Chem. Soc.* **2005**, *127*, 5758−5759.

(26) Scholten, J. D.; Ebeling, G.; Dupont, J. On the Involvement of NHC Carbenes in Catalytic Reactions by Iridium Complexes, Nanoparticle and Bulk Metal Dispersed in Imidazolium Ionic Liquids. *Dalton Trans.* **2007**, 5554−5560.

(27) Huang, R. T. W.; Wang, W. C.; Yang, R. Y.; Lu, J. T.; Lin, I. J. B. Liquid Crystals of Gold(I) *N*-Heterocyclic Carbene Complexes. *Dalton Trans.* **2009**, 7121−7131.

(28) Hurst, E. C.; Wilson, K.; Fairlamb, I. J. S.; Chechik, V. *N*-Heterocyclic Carbene Coated Metal Nanoparticles. *New J. Chem.* **2009**, *33*, 1837−1840.

(29) Vignolle, J.; Tilley, T. D. *N*-Heterocyclic Carbene-Stabilized Gold Nanoparticles and their Assembly into 3D Superlattices. *Chem. Commun.* **2009**, 7230−7232.

(30) Aslanov, L. A.; Zakharov, V. N.; Zakharov, M. A.; Kamyshny, A. L.; Magdassi, Sh.; Yatsenko, A. V. Stabilization of Silicon Nanoparticles by Carbenes. *Russ. J. Coord. Chem.* **2010**, *36*, 330−332.

(31) Choi, J.; Kang, N.; Yang, H. Y.; Kim, H. J.; Son, S. U. Colloidal Synthesis of Cubic-Phase Copper Selenide Nanodiscs and Their Optoelectronic Properties. *Chem. Mater.* **2010**, *22*, 3586−3588.

(32) Ranganath, K. V. S.; Kloesges, J.; Schäfer, A. H.; Glorius, F. Asymmetric Nanocatalysis: *N*-Heterocyclic Carbenes as Chiral Modifiers of Fe$_3$O$_4$/Pd Nanoparticles. *Angew. Chem., Int. Ed.* **2010**, *49*, 7786−7789.

(33) Lara, P.; Rivada-Wheelaghan, O.; Conejero, S.; Poteau, R.; Philippot, K.; Chaudret, B. Ruthenium Nanoparticles Stabilized by *N*-Heterocyclic Carbenes: Ligand Location and Influence on Reactivity. *Angew. Chem., Int. Ed.* **2011**, *50*, 12080−12084.

(34) Gonzales-Galves, D.; Lara, P.; Rivada-Wheelaghan, O.; Conejero, S.; Chaudret, B.; Philippot, K.; van Leeuwen, P. W. N. M. NHC-Stabilized Ruthenium Nanoparticles as New Catalysts for the Hydrogenation of Aromatics. *Catal. Sci. Technol.* **2013**, *3*, 99−105.

(35) Serpell, C. J.; Cookson, J.; Thompson, A. L.; Brown, C. M.; Beer, P. D. Haloaurate and Halopalladate Imidazolium Salts: Structures, Properties, and Use as Precursors for Catalytic Metal Nanoparticles. *Dalton Trans.* **2013**, *42*, 1385−1393.

(36) Song, S. G.; Satheeshkumar, C.; Park, J.; Ahn, J.; Premkumar, T.; Lee, Y.; Song, C. *N*-Heterocyclic Carbene-Based Conducting Polymer−Gold Nanoparticle Hybrids and Their Catalytic Application. *Macromolecules* **2014**, *47*, 6566−6571.

(37) Baquero, E. A.; Tricard, S.; Flores, J. C.; de Jesús, E.; Chaudret, B. Highly Stable Water-Soluble Platinum Nanoparticles Stabilized by Hydrophilic *N*-Heterocyclic Carbenes. *Angew. Chem., Int. Ed.* **2014**, *53*, 13220−13224.

(38) Liu, H.-X.; He, X.; Zhao, L. Metallamacrocycle-Modified Gold Nanoparticles: A New Pathway for Surface Functionalization. *Chem. Commun.* **2014**, *50*, 971−974.

(39) Richter, C.; Schaepe, K.; Glorius, F.; Ravoo, B. J. Tailor-made *N*-Heterocyclic Carbenes for Nanoparticle Stabilization. *Chem. Commun.* **2014**, *50*, 3204−3207.

(40) Rodriguez-Castillo, M.; Laurencin, D.; Tielens, F.; van der Lee, A.; Clément, S.; Guari, Y.; Richeter, S. Reactivity of Gold Nanoparticles Towards *N*-Heterocyclic Carbenes. *Dalton Trans.* **2014**, *43*, 5978−5982.

(41) Crespo, J.; Guari, Y.; Ibarra, A.; Larionova, J.; Lasanta, T.; Laurencin, D.; López-de-Luzuriaga, J. M.; Monge, M.; Olmos, M. E.; Richeter, S. Ultrasmall NHC-Coated Gold Nanoparticles Obtained through Solvent Free Thermolysis of Organometallic Au(I) Complexes. *Dalton Trans.* **2014**, *43*, 15713−15718.

(42) MacLeod, M. J.; Johnson, J. A. PEGylated N-Heterocyclic Carbene Anchors Designed to Stabilize Gold Nanoparticles in Biologically Relevant Media. *J. Am. Chem. Soc.* **2015**, *137*, 7974−7977.

(43) Ferry, A.; Schaepe, K.; Tegeder, P.; Richter, C.; Chepiga, K. M.; Ravoo, B. J.; Glorius, F. Negatively Charged *N*-Heterocyclic Carbene-Stabilized Pd and Au Nanoparticles and Efficient Catalysis in Water. *ACS Catal.* **2015**, *5*, 5414−5420.

(44) Zhukhovitskiy, A. V.; MacLeod, M. J.; Johnson, J. A. Carbene Ligands in Surface Chemistry: From Stabilization of Discrete Elemental Allotropes to Modification of Nanoscale and Bulk Substrates. *Chem. Rev.* **2015**, *115*, 11503−11532.

(45) Weidner, T.; Baio, J. E.; Mundstock, A.; Große, C.; Karthäuser, S.; Bruhn, C.; Siemeling, U. NHC-Based Self-Assembled Monolayers on Solid Gold Substrates. *Aust. J. Chem.* **2011**, *64*, 1177−1179.

(46) Zhukhovitskiy, A. V.; Mavros, M. G.; Van Voorhis, T.; Johnson, J. A. Addressable Carbene Anchors for Gold Surfaces. *J. Am. Chem. Soc.* **2013**, *135*, 7418−7421.

(47) Crudden, C. M.; Horton, J. H.; Ebralidze, I. I.; Zenkina, O. V.; McLean, A. B.; Drevniok, B.; She, Z.; Kraatz, H.-B.; Mosey, N. J.; Seki, T.; Keske, E. C.; Leake, J. D.; Rousina-Webb, A.; Wu, G. Ultra Stable Self-Assembled Monolayers of *N*-Heterocyclic Carbenes on Gold. *Nat. Chem.* **2014**, *6*, 409−414.

(48) Benhamou, L.; Chardon, E.; Lavigne, G.; Bellemin-Laponnaz, S.; César, V. Synthetic Routes to *N*-Heterocyclic Carbene Precursors. *Chem. Rev.* **2011**, *111*, 2705−2733.

(49) Nelson, D. J.; Nolan, S. P. Quantifying and Understanding the Electronic Properties of *N*-Heterocyclic Carbenes. *Chem. Soc. Rev.* **2013**, *42*, 6723−6753.

(50) For gold complexes, see Pyykkö, P.; Runeberg, N. Comparative Theoretical Study of *N*-Heterocyclic Carbenes and Other Ligands Bound to Au^I. *Chem. - Asian J.* **2006**, *1*, 623−628.

(51) Ling, X.; Schaeffer, N.; Roland, S.; Pileni, M.-P. Nanocrystals: Why Do Silver and Gold *N*-Heterocyclic Carbene Precursors Behave Differently ? *Langmuir* **2013**, *29*, 12647−12656.

(52) Ling, X.; Roland, S.; Pileni, M.-P. Superior Oxygen Stability of *N*-Heterocyclic Carbene-Coated Au Nanocrystals. *Langmuir* **2015**, *31*, 12873−12882.

(53) Ling, X.; Roland, S.; Pileni, M.-P. Supracrystals of *N*-Heterocyclic Carbene-Coated Au Nanocrystals. *Chem. Mater.* **2015**, *27*, 414−423.

(54) Zheng, N.; Fan, J.; Stucky, G. D. One-Step One-Phase Synthesis of Monodisperse Noble-Metallic Nanoparticles and Their Colloidal Crystals. *J. Am. Chem. Soc.* **2006**, *128*, 6550−6551.

(55) Goubet, N.; Richardi, J.; Albouy, P.-A.; Pileni, M.-P. Which Forces Control Supracrystal Nucleation in Organic Media ? *Adv. Funct. Mater.* **2011**, *21*, 2693−2704.

(56) For example, see Pytkowicz, J.; Roland, S.; Mangeney, P.; Meyer, G.; Jutand, A. Chiral Diaminocarbene Palladium(II) Complexes: Synthesis, Reduction to Pd(0) and Activity in the Mizoroki-Heck Reaction as Recyclable Catalyst. *J. Organomet. Chem.* **2003**, *678*, 166−179.

(57) Tsui, E. Y.; Müller, P.; Sadighi, J. R. Reactions of a Stable Monomeric Gold(I) Hydride Complex. *Angew. Chem., Int. Ed.* **2008**, *47*, 8937−8940.

(58) Ling, X. Unpublished experiments. Ph.D. thesis, UPMC-Univ Paris 6, 2015.

(59) For Au(111) coated with linear alkanethiols, the maximum S/ Au was shown to be 1:3. See Djebaili, T.; Richardi, J.; Abel, S.; Marchi, M. Atomistic Simulations of the Surface Coverage of Large Gold Nanocrystals. *J. Phys. Chem. C* **2013**, *117*, 17791−17800.

(60) Cortés, E.; Rubert, A. A.; Benitez, G.; Carro, P.; Vela, M. E.; Salvarezza, R. C. Enhanced Stability of Thiolate Self-Assembled Monolayers (SAMs) on Nanostructured Gold Substrates. *Langmuir* **2009**, *25*, 5661−5666.

(61) Wan, Y. F.; Goubet, N.; Albouy, P. A.; Schaeffer, N.; Pileni, M.-P. Hierarchy in Au Nanocrystal Ordering in a Supracrystal: II. The Control of Inter-Nanocrystal Distances. *Langmuir* **2013**, *29*, 13576−13581.

(62) For similar structures observed by XPS, see Castner, D. G.; Hinds, K.; Grainger, D. W. X-ray Photoelectron Spectroscopy Sulfur 2p Study of Organic Thiol and Disulfide Binding Interactions with Gold Surfaces. *Langmuir* **1996**, *12*, 5083−5086.

(63) Park, E. D.; Lee, J. S. Effects of Pretreatment Conditions on CO Oxidation over Supported Au Catalysts. *J. Catal.* **1999**, *186*, 1−11.

(64) Venezia, A. M.; Pantaleo, G.; Longo, A.; Di Carlo, G.; Casaletto, M. P.; Liotta, F. L.; Deganello, G. Relationship between Structure and CO Oxidation Activity of Ceria-Supported Gold Catalysts. *J. Phys. Chem. B* **2005**, *109*, 2821−2827.

(65) Casaletto, M. P.; Longo, A.; Martorana, A.; Prestianni, A.; Venezia, A. M. XPS Study of Supported Gold Catalysts: The Role of Au^0 and Au$^{+\delta}$ Species as Active Sites. *Surf. Interface Anal.* **2006**, *38*, 215−218.

(66) Krommenhoek, P. J.; Wang, J.; Hentz, N.; Johnston-Peck, A. C.; Kozek, K. A.; Kalyuzhny, G.; Tracy, J. B. Bulky Adamantanethiolate and Cyclohexanethiolate Ligands Favor Smaller Gold Nanoparticles with Altered Discrete Sizes. *ACS Nano* **2012**, *6*, 4903−4911.

(67) Oxygen plasma was previously used to assess the resistance of silver nanocrystals in different types of 2D self-assemblies. Klecha, E.; Arfaoui, I.; Richardi, J.; Ingert, D.; Pileni, M.-P. 2D Silver Nanocrystal Ordering Modulated by Various Substrates and Revealed Using Oxygen Plasma Treatment. *Phys. Chem. Chem. Phys.* **2011**, *13*, 2953−2962.

(68) Salzemann, C.; Zhai, W.; Goubet, N.; Pileni, M.-P. How to Tune the Au Internanocrystal Distance in Two-Dimensional Self-Ordered Superlattices. *J. Phys. Chem. Lett.* **2010**, *1*, 149−154.

(69) Lavrich, D. J.; Wetterer, S. M.; Bernasek, S. L.; Scoles, G. Physisorption and Chemisorption of Alkanethiols and Alkyl Sulfides on Au(111). *J. Phys. Chem. B* **1998**, *102*, 3456−3465.

(70) Nuzzo, R. G.; Dubois, L. H.; Allara, D. L. Fundamental Studies of Microscopic Wetting on Organic Surfaces. 1. Formation and Structural Characterization of a Self-Consistent Series of Polyfunctional Organic Monolayers. *J. Am. Chem. Soc.* **1990**, *112*, 558−569.

(71) Ristig, S.; Kozlova, D.; Meyer-Zaika, W.; Epple, M. An Easy Synthesis of Autofluorescent Alloyed Silver−Gold Nanoparticles. *J. Mater. Chem. B* **2014**, *2*, 7887−7895.

(72) As similarly noted with SAMs: Cortés, E.; Rubert, A. A.; Benitez, G.; Carro, P.; Vela, M. E.; Salvarezza, R. C. Enhanced Stability of Thiolate Self-Assembled Monolayers (SAMs) on Nanostructured Gold Substrates. *Langmuir* **2009**, *25*, 5661−5666 and references therein..

(73) Talapin, D. V.; Lee, J.-S.; Kovalenko, M. V.; Shevchenko, E. V. Prospects of Colloidal Nanocrystals for Electronic and Optoelectronic Applications. *Chem. Rev.* **2010**, *110*, 389−458.

(74) Auer, S.; Frenkel, D. Suppression of Crystal Nucleation in Polydisperse Colloids due to Increase of the Surface Free Energy. *Nature* **2001**, *413*, 711−713.

(75) Wan, Y. F.; Goubet, N.; Albouy, P. A.; Pileni, M.-P. Hierarchy in Au Nanocrystal Ordering in Supracrystals: A Potential Approach to Detect new Physical Properties. *Langmuir* **2013**, *29*, 7456−7463.

(76) Yang, N.; Yang, Z.; Held, M.; Bonville, P.; Albouy, P. A.; Lévy, R.; Pileni, M.-P. Dispersion of Hydrophobic Co Supracrystal in Aqueous Solution. *ACS Nano* **2016**, *10*, 2277−2286.

(77) Yang, Z.; Altantzis, T.; Zanaga, D.; Bals, S.; Van Tendeloo, G.; Pileni, M.-P. Supracrystalline Colloidal Eggs: Epitaxial Growth and Freestanding Three-Dimensional Supracrystals in Nanoscaled Colloidosomes. *J. Am. Chem. Soc.* **2016**, *138*, 3493−3500.

(78) Pileni, M.-P. Nanocrystals Self-Assemblies: Fabrication and Collective Properties. *J. Phys. Chem. B* **2001**, *105*, 3358−3371.

(79) Pileni, M.-P. Supracrystals of Inorganic Nanocrystals: An Open Challenge for New Physical Properties. *Acc. Chem. Res.* **2008**, *41*, 1799−1809.

(80) Gauvin, M.; Wan, Y.; Arfaoui, I.; Pileni, M.-P. Mechanical Properties of Au Supracrystals Tuned by Flexible Ligand Interaction. *J. Phys. Chem. C* **2014**, *118*, 5005−5012.

(81) Wei, J.; Schaeffer, N.; Albouy, P.-A.; Pileni, M.-P. Surface Plasmon Resonance Properties of Silver Nanocrystals Differing in Size and Coating Agent Ordered in 3D Supracrystals. *Chem. Mater.* **2015**, *27*, 5614−5621.

(82) Ross, M. B.; Ku, J. C.; Vaccarezza, V. M.; Schatz, G. C.; Mirkin, C. A. Nanoscale Form Dictates Mesoscale Function in Plasmonic DNA−Nanoparticle Superlattices. *Nat. Nanotechnol.* **2015**, *10*, 453−458.

(83) Zhang, C.; Zhou, Y.; Merg, A.; Song, C.; Schatz, G. C.; Rosi, N. L. Hollow Spherical Gold Nanoparticle Superstructures with Tunable

Diameters and Visible to Near-Infrared Extinction. *Nanoscale* **2014**, *6*, 12328−12332.

(84) Hedayati, M.; Faupel, F.; Elbahri, M. Review of Plasmonic Nanocomposite Metamaterial Absorber. *Materials* **2014**, *7*, 1221−1248.

(85) Tao, A. R.; Ceperley, D. P.; Sinsermsuksakul, P.; Neureuther, A. R.; Yang, P. Self-Organized Silver Nanoparticles for Three-Dimensional Plasmonic Crystals. *Nano Lett.* **2008**, *8*, 4033−4038.

(86) The absorption spectrum of Au supracrystals dispersed in aqueous solution shows a large peak at very low energy (<1 eV). This peak is shifted to the red on increasing the supracrystal size. Note that the signature of the LSRP remains at around 560−590 nm. Wang, N.; Pileni, M.-P. *Personal communication*.

(87) Pileni, M.-P. Nano-supracrystallinity. *EPL* **2015**, *109*, 58001−58007.